SUBMARINE LANDSLIDE-INDUCED TSUNAMI MODEL USING NONLINEAR SHALLOW WATER EQUATIONS IN *(b, s)* COORDINATE AND EXTENDED BOUSSINESQ EQUATIONS

MÔ HÌNH SẠT LỞ ĐẤT ĐÁY BIỂN TẠO SÓNG THẦN DÙNG HỆ PHƯƠNG TRÌNH PHI TUYẾN NƯỚC NÔNG VỚI HỆ TỌA ĐỘ (b, s) VÀ HỆ PHƯƠNG TRÌNH BOUSSINESQ MỞ RỘNG

Van Khoi Pham[1], Changhoon Lee[2], Van Nghi Vu[3]
[1,2]Sejong University, Seoul, South Korea,
[3]Ho Chi Minh City University of Transport, Vietnam

***Abstract**: Due to earthquakes or other earth phenomena, a landslide occurs underwater and thus tsunami is generated and propagates without much energy loss even at long distances. After the tsunami arrives at the coastline, it may cause serious casualties. The submarine landslide and the tsunami should be analyzed together to predict the inter-connected phenomena. In this study, we simulate submarine landslide using the one-dimensional conservative form of the nonlinear shallow water equations (NSWE) in (b, s) coordinate* [1]. *Where b and s are the elevations of debris bottom and surface, respectively. The NSWE is discretized using the finite volume method employing the Harten-Lax-van Leer (HLL) approximate Riemann solver and the total variation diminishing (TVD) limiter to deal with numerical discontinuities. To simulate landslide-induced tsunami, we use the one-dimensional form of the extended Boussinesq equations considering time-varying debris surfaces* [2] *which extends Madsen and Sorensen's extended Boussinesq equations* [3]. *An Adams-Bashforth-Moulton predictor-corrector scheme is used to discretize the extended Boussinesq equations in time. The submarine landslide and the induced tsunami are simulated in some test cases.*

***Keywords**: Submarine landslide, tsunami, nonlinear shallow water equations, extended Boussinesq equations, numerical simulation.*

***Classification code:** 11.2*

***Tóm tắt:** Do động đất hoặc các hiện tượng địa chấn khác, sạt lở đất xuất hiện dưới đáy biển. Do đó, sóng thần được hình thành, lan truyền nhanh và không bị tổn hao năng lượng. Khi sóng thần lan truyền tới đường bờ, nó có thể gây ra thảm họa đối với đất liền. Sạt lở đất đáy biển và sóng thần cần được phân tích song song để có thể dự đoán những hiện tượng phức tạp của quá trình này. Trong nghiên cứu, nhóm tác giả mô phỏng sạt lở đất đáy biển dùng hệ phương trình phi tuyến nước nông một chiều dạng bảo toàn với hệ tọa độ (b, s) [1]. Trong đó b và s tương ứng là chiều cao đáy và chiều cao bề mặt của đáy biển sạt lở. Hệ phương trình phi tuyến nước nông được rời rạc hóa bằng phương pháp thể tích hữu hạn, trong đó áp dụng lời giải xấp xỉ Harten-Lax-van Leer (HLL) và công tắc chuyển đổi (TVD) cho thành phần thông lượng để có thể giải bài toán phương pháp số không liên tục. Nhằm mô phỏng sạt lở đất tạo sóng thần, nhóm đã dùng hệ phương trình Boussinesq một chiều có kể đến bề mặt đáy biển biến đổi theo thời gian [2]. Đây cũng chính là dạng hệ phương trình Boussinesq mở rộng của Madsen và Sorensen [3]. Phương pháp dự đoán - hiệu chỉnh của Adams – Bashforth - Moulton được dùng để rời rạc hóa hệ phương trình Boussinesq theo bước thời gian. Và sạt lở đất đáy biển và sóng thần được mô phỏng với một vài trường hợp cụ thể.*

***Từ khóa:** Sạt lở đất đáy biển, sóng thần, hệ phương trình phi tuyến nước nông, hệ phương trình Boussinesq mở rộng, mô phỏng số.*

***Mã phân loại:** 11.2*

1. Introduction

To date, the submarine landslide-induced tsunami is a tremendous challenge topic for ocean researchers. On March 11th, 2011, about 18,000 people died due to the tsunami and earthquake in Tohoku, Japan. People found that the submarine landslide source may contribute to the tsunami which had a wave height of 40 m near the coastline [4]. Recently, due to the Anak Krakatau volcano collapse, a tsunami occurred and killed approximately 430 people in Indonesia [5]. In Quang Nam province, Vietnam, a tsunami due to a subaerial-submarine landslide killed

one person and destroyed parts of the village near the Truong river on November 5th, 2017 [6]. Comparing to the tsunami due to earthquakes, the tsunami due to landslides may cause a higher wave amplitude and a shorter wavelength [7]. Thus, many researchers make efforts to predict this inter-connected phenomenon.

Until now, regarding the submarine landslide-induced tsunami models, it can be divided into two approaches. One approach is to assume debris surface in an elliptic shape and consider the bottom variation in the Boussinesq equations [8, 9]. In reality, the debris surface is not elliptic-shaped and also changes depending on the bottom slope and side slopes. The other approach is to simulate debris flow using the NSWE and considers the bottom variation in the NSWE [10–12]. In reality, the landslide-induced tsunami has not only long waves but also short waves as which cannot be simulated accurately with the NSWE.

In this study, we simulate debris flow using the NSWE and consider the bottom variation in the Boussinesq equations. Then, the surface of the debris can be accurately simulated, and also short wave components of the tsunami can be accurately simulated. Therefore, the submarine landslide is simulated as the debris flow (or the deformable landslide) using NSWE employing the finite volume method which can deal with the discontinuity in landslide simulation. Furthermore, the tsunami is simulated using Boussinesq equations which include the bottom variation in time and dispersive terms to deal with the short waves of submarine landslide-induced tsunami waves.

2. Submarine landslide-induced tsunami model

This section introduces governing equations in the present model: the NSWE for the submarine landslide model and the extended Boussinesq equations for the water wave model.

2.1. Equations for submarine landslide

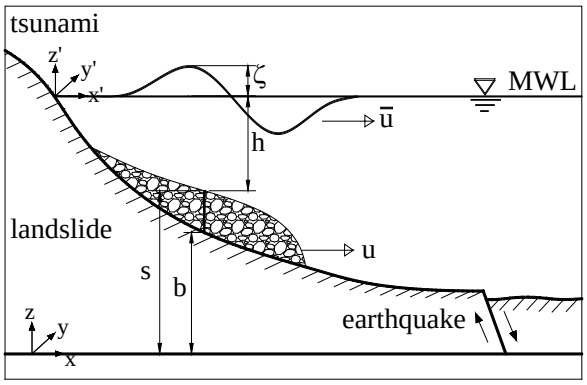

Figure 1. *Computational domain of submarine landslide-induced tsunami.*

The one-dimensional conservative form of NSWE for landslides in (b, s) coordinates is given by

$$\frac{\partial U}{\partial t}+\frac{\partial F(U)}{\partial x}=H(U) \tag{1}$$

Where:

$$U=\begin{pmatrix} s \\ (s-b)u \end{pmatrix} \tag{2}$$

$$F(U)=\begin{pmatrix} (s-b)u \\ (s-b)u^2+\frac{1}{2}g(s-b)^2 \end{pmatrix} \tag{3}$$

$$H(U)=\begin{bmatrix} 0 \\ g(s-b)\left(S_0-\mu\cos\theta-\frac{n^2u|u|}{(s-b)^{4/3}}\right) \end{bmatrix} \tag{4}$$

Where s and b are the elevations of debris surface and bottom, respectively, u is the depth-averaged debris particle velocity in the x-direction. S_0 ($=-\partial b/\partial x=\tan\theta$) is the bottom slope ($\theta$ is the bottom slope angle), μ ($=\tan\phi$) and n is the effective friction coefficient (ϕ is the internal friction angle), and the Manning's roughness coefficient which considers the debris flow resistance. The variables are shown in figure 1. Because the (b, s) coordinates are generally defined to use the z-axis vertically, the time-varying debris surface can be easily converted to the time-varying water depth. But, the debris depth which is normal to the slope is difficult to convert to the water depth in the water wave model which uses the (h, ζ) coordinate [5], [10].

2.2. Equations for a motion of tsunami

The one-dimensional extended Boussinesq equations with time-varying bottom terms are used to simulate tsunami [2]:

$$\frac{\partial \zeta}{\partial t}+\frac{\partial}{\partial x}\left[\left(h+\zeta\right)\overline{u}\right]+\frac{\partial h}{\partial t}=0 \quad (5)$$

$$\frac{\partial \overline{u}}{\partial t}+g\frac{\partial \zeta}{\partial x}+\overline{u}\frac{\partial \overline{u}}{\partial x}+\frac{h^2}{6}\frac{\partial^3 \overline{u}}{\partial x^2 \partial t}-\left(\frac{1}{2}+\gamma\right)h\frac{\partial^2}{\partial x^2}\left(h\frac{\partial \overline{u}}{\partial t}\right)-\gamma g h\frac{\partial^2}{\partial x^2}\left(h\frac{\partial \zeta}{\partial x}\right)-\frac{h}{2}\frac{\partial^3 h}{\partial x \partial t^2}=0 \quad (6)$$

Where $\overline{u}$ and ζ are the depth-averaged velocity in the x-direction and the surface elevation of water waves, respectively, $h(x,t)$ is the water depth changing in time and space as shown in Figure 1, γ (=1/15) is the tuning parameter to extend the applicability of the model to deeper waters [2, 3, 13, 14]. If we neglect the terms $\partial h/\partial t$ and $h\left(\partial^3 h/\partial x \partial t^2\right)/2$ in Eqs. (5) and (6), respectively, then Lee and Vu's extended Boussinesq equations [2] are reduced to Madsen and Sorensen's extended Boussinesq equations [3].

3. Numerical Schemes

3.1. Numerical scheme for submarine landslide model

To deal with the discontinuity problem which is seriously important in the submarine landslide simulation, the hybrid finite volume-finite difference scheme is applied to discretize the spatial derivatives of the one-dimensional governing equations (1). The power finite volume scheme is applied to solve the numerical flux terms $F(U)$ and the finite difference scheme is applied for the bottom slope term in the source term $H(U)$. The flux interfaces are computed using the weighted averaged flux (WAF) which employs the TVD limiter function to deal with the discontinuity problem. The limiter function using for all researches is the van Leer limiter function which is also used in the FUNWAVE-TVD [15]. In the star region, the HLL approximate Riemann solver is used to compute the flux interface. Other details in the finite volume scheme can be seen in [1]. To discretize the equations (1) in time, the explicit three-stage three-order Runge-Kutta [16–19] is using in this model.

3.2. Numerical scheme for a tsunami model

The one-dimensional water wave governing equations (5) and (6) can be discretized using the well-known finite difference method following FUNWAVE 1.0 [20]. For time integration, a set of third-order Adams-Basforth predictor scheme and fourth-order Adams-Moulton corrector scheme is used. For spatial derivatives, the first-order terms are discretized up to $O(\Delta x^4)$ and the higher-order terms which are dispersive terms are discretized up to $O(\Delta x^2)$ [21]. Other details in the finite difference method can be found in [14], [22].

4. Model verification

The small-scale landslide described in [23] is presented in this section. The computational domain is 4 m long, from x = -1 m to x = 3 m as shown in figure 2. The water depth is 0.1 m at the upper part and increases to 1.6 m at the lower part of the domain. A sand box with dimensions of 0.65 m x 0.65 m is installed on the steep slope of 45^o by a gate. The sand mean density is 1950 kg/m^3. After opening the gate, the sand freely falls down on the slope then the water surface fluctuates which is called as the tsunami. For landslide resistance properties, the Manning's coefficient and the effective friction coefficient are taken into account of n = 0.56 m$^{-1/3}$s and μ =1, respectively.

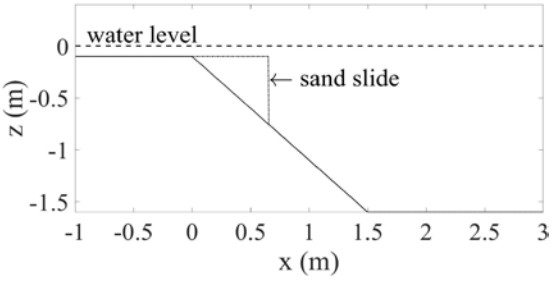

***Figure 2**.Computational domain of laboratory submarine landslide [23].*

Figure 3(a) and figure 3(b) compare water surface elevations of the present simulation results with the experimental data [23] at t = 0.4 s and at t = 0.8 s.

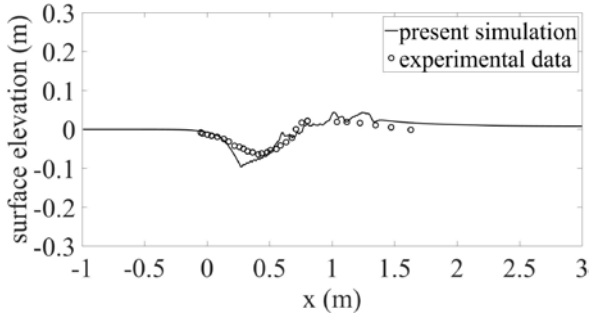

(a)

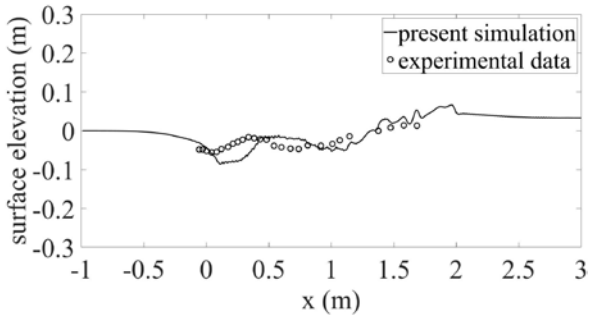

(b)

Figure 3. *Elevations of tsunami due to submarine sand landslides: (a) t = 0.4 s, (b) t = 0.8 s.*

On the whole, the present simulation results show good agreements with the experimental data. Due to very short wavelengths, the water surface elevations are very noisy. Thus, in this present verification, we use the smoothing technique [1] with a span of 33 to filter the numerical results.

5. Model applications and discussions

We extend model applications to a larger-scale, i.e., the real domain of the submarine landslide-induced tsunami as shown in figure 4.

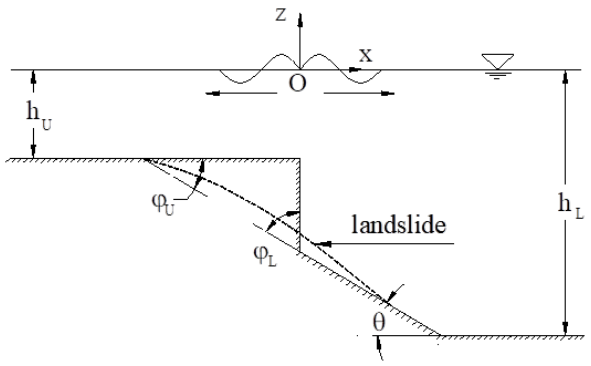

Figure 4*. Computational domain of landslide-induced tsunami application.*

In figure 4, the upper depth is h_U = 50 m and the lower depth is h_L = 300 m. The debris in a triangular shape with the upper angle of φ_U = 20º, the lower angle of φ_L = 70º, and the horizontal length of 210 m slides down on the slope of θ = 20º. For resistance properties, the internal friction angle of ϕ = 24º and the Manning's coefficient of n = 0.12 $m^{-1/3}s$ are used in this study. Figures 5 (a) - (c) show numerical results of submarine landslide and the induced tsunami at t = 1 s, 10 s, 50 s. In figure 5, the solid lines at the upper and lower parts are the tsunami and the submarine debris surface, respectively. And the dashed and dash-dotted lines are the bottom and the initial debris surface, respectively.

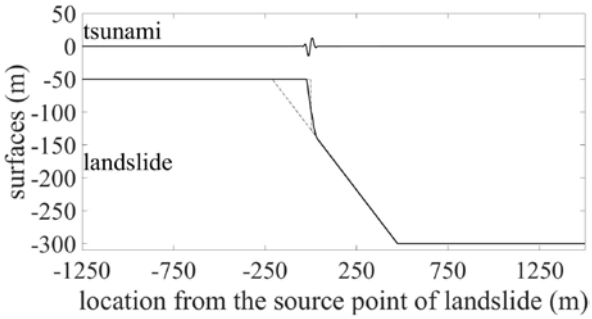

(a)

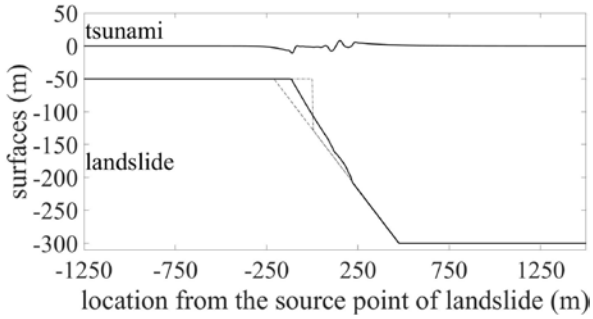

(b)

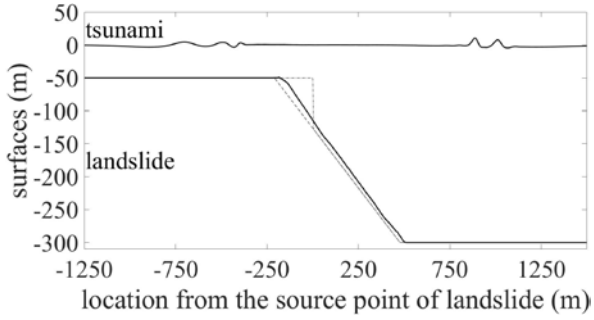

(c)

Figure 5*. Elevations of submarine landslide and the induced tsunami at different times: (a) t=1 s, (b) t = 10 s, (c) t = 50 s.*

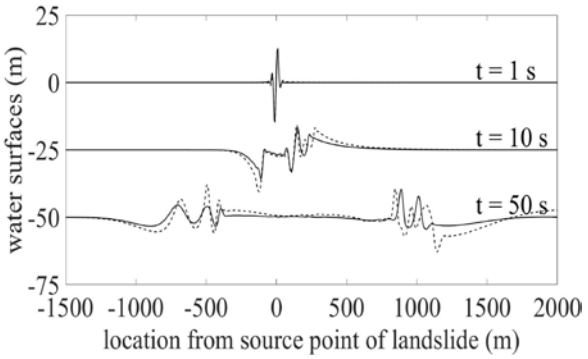

(a)

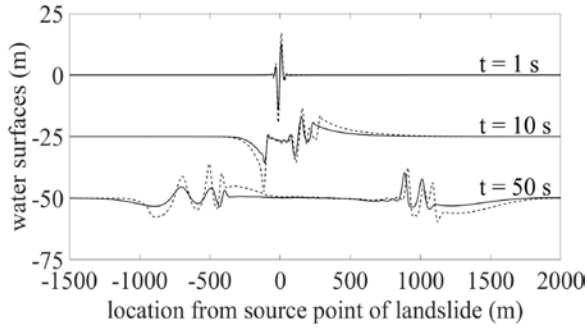

(b)

***Figure 6**. Elevations of tsunami at t = 1 s, 10 s, 50 s: (a) different internal friction angles (---: $\phi = 24^o$, - - -: $\phi = 6^o$), (b) different bottom slope angles (---: $\theta = 20^o$, - - -: $\theta = 25^o$).*

Just after the landslide, water responds quickly with a high wave amplitude of 15 m (see figure 5(a)). As time goes by, two components are moving in opposite directions. One component propagating to the deeper region has wave amplitudes not varying smaller even though it moves deeper zone. It is because the bottom moves in the direction of the deeper zone which gives energy. The other component propagating to the shallower region has wave amplitudes smaller than the component in the deeper region. It is because there is no energy input to the shallower zone (see figures 5(b), (c)). For sensitivity analysis, two important parameters are considered in this study. That is, the internal friction angle decreases from 24º to 6º (see figure 6(a)) or the bottom slope angle increases from 20º to 25º (see figure 6(b)). As shown in figure 6(a), when the internal friction angle decreases, the debris resistance decreases, and thus the submarine landslide velocity increases, and therefore the wave amplitude increases, especially at the left-hand side of the domain due to the shoaling effect. Similarly, the wave amplitudes at the left- and right-hand side components are higher when the bottom slope angle increases as shown in Figure 6(b). These results are physically reasonable and were mentioned in [22].

6. Conclusions

In this study, the new submarine landslide-induced tsunami model is developed using the NSWE and the extended Boussinesq equations. The submarine landslide is simulated using the NSWE in (b, s) coordinates which are defined in the vertical direction, then the debris surfaces can be conveniently converted to the time-varying water depths. The tsunami is simulated using the extended Boussinesq equations which include the time-varying water depths from the landslide simulation results and the dispersive terms in the equations consider the short waves which exist in the landslide-induced tsunami. The model is verified well with the experimental data. Further, the model is simulated successfully in the horizontally one-dimensional domain with different internal frictional angles or bottom slopes to see these effects in the physical senses. The wave run-up and horizontally two-dimensional models will be developed to be applied in real submarine landslide-induced tsunami❑

References

[1] V. K. Pham, C. Lee, and V. N. Vu (2019), *Numerical Simulation of Subaerial and Submarine Landslides Using the Finite Volume Method in the Shallow Water Equations with (b, s) Coordinate*, J Korean Soc Coast Ocean Eng, vol. 31, no. 4, pp. 229–239, Aug. 2019, DOI: 10.9765/KSCOE.2019.31.4.229;

[2] C. Lee and V. N. Vu (2015), *Development of extended Boussinesq equations to simulate tsunami generation and propagation*, Proceedings of Coastal and Ocean Engineering in Korea, South Korea, pp. 1–3, 2015;

[3] P. A. Madsen and O. R. Sørensen (1992), *A new form of the Boussinesq equations with improved linear dispersion characteristics. Part 2. A slowly-varying bathymetry*, Coastal Engineering, vol. 18, no. 3–4, pp. 183–204, Dec. 1992, DOI: 10.1016/0378-3839(92)90019-Q;

[4] D. R. Tappin et al. (2014), *Did a submarine landslide contribute to the 2011 Tohoku tsunami?*, *Marine Geology*, vol. 357, pp. 344–361, Nov. 2014,
DOI: 10.1016/j.margeo.2014.09.043;

[5] A. Paris, P. Heinrich, R. Paris, and S. Abadie (2020), *The December 22, 2018, Anak Krakatau, Indonesia, Landslide and Tsunami: Preliminary Modeling Results*, Pure Appl. Geophys., vol. 177, no. 2, pp. 571–590, Feb. 2020,
DOI: 10.1007/s00024-019-02394-y;

[6] D. M. Duc et al. (2020), *Analysis and modeling of a landslide-induced tsunami-like wave across the Truong river in Quang Nam province, Vietnam*, Landslides, vol. 17, no. 10, pp. 2329–2341, Oct. 2020,
DOI: 10.1007/s10346-020-01434-2;

[7] S. Yavari-Ramshe and B. Ataie-Ashtiani (2016), *Numerical modeling of subaerial and submarine landslide-generated tsunami waves—recent advances and future challenges*, Landslides, vol. 13, no. 6, pp. 1325–1368, Dec. 2016,
DOI: 10.1007/s10346-016-0734-2;

[8] P. Lynett and P. L.-F. Liu (2002), *A Numerical Study of Submarine-Landslide-Generated Waves and Run-Up*, Proceedings: Mathematical, Physical and Engineering Sciences, vol. 458, no. 2028, pp. 2885–2910, 2002;

[9] D. Dutykh and H. Kalisch (2013), *Boussinesq modeling of surface waves due to underwater landslides*, Nonlin. Processes Geophys., vol. 20, no. 3, pp. 267–285, May 2013,
DOI: 10.5194/npg-20-267-2013;

[10] S. Assier-Rzadkiewicz, P. Heinrich, P. C. Sabatier, B. Savoye, and J. F. Bourillet (2000), *Numerical Modelling of a Landslide-generated Tsunami: The 1979 Nice Event*, Pure appl. *geophys.*, vol. 157, no. 10, pp. 1707–1727, Oct. 2000,
DOI: 10.1007/PL00001057;

[11] P. Heinrich, A. Piatanesi, and H. Hebert (2001), *Numerical modeling of tsunami generation and propagation from submarine slumps: the 1998 Papua New Guinea event*, Geophysical Journal International, pp. 97–111, 2001;

[12] K. Sassa, K. Dang, H. Yanagisawa, and B. He (2016), *A new landslide-induced tsunami simulation model and its application to the 1792 Unzen-Mayuyama landslide-and-tsunami disaster*, Landslides, vol. 13, no. 6, pp. 1405–1419, Dec. 2016,
DOI: 10.1007/s10346-016-0691-9;

[13] T. T. Huynh, C. Lee, and S. J. Ahn (2017), *Numerical Simulation of Wave Overtopping on a Porous Breakwater Using Boussinesq Equations*, J Korean Soc Coast Ocean Eng, vol. 29, no. 6, pp. 326–334, Dec. 2017,
DOI: 10.9765/KSCOE.2017.29.6.326;

[14] V. N. Vu, C. Lee, and T.-H. Jung (2018), *Extended Boussinesq equations for waves in porous media*, *Coastal Engineering*, vol. 139, pp. 85–97, Sep. 2018,
DOI: 10.1016/j.coastaleng.2018.04.023;

[15] F. Shi, J. T. Kirby, B. Tehranirad, and J. C. Harris (2016), *FUNWAVE-TVD Fully Nonlinear Boussinesq Wave Model with TVD Solver - Documentation and User's Manual (Version 3.0), Report NO. CACR-11-03*, Center for Applied Coastal Research, Univ. of Delaware, Dec. 2016;

[16] C.-W. Shu and S. Osher (1988), E*fficient implementation of essentially non-oscillatory shock-capturing schemes*, Journal of Computational Physics, vol. 77, no. 2, pp. 439–471, Aug. 1988,
DOI: 10.1016/0021-9991(88)90177-5;

[17] S. Gottlieb, C.-W. Shu, and E. Tadmor (2001), *Strong Stability-Preserving High-Order Time Discretization Methods*, SIAM Rev., vol. 43, no. 1, pp. 89–112, Jan. 2001,
DOI: 10.1137/S003614450036757X;

[18] R. J. Spiteri and S. J. Ruuth (2002), *A New Class of Optimal High-Order Strong-Stability-Preserving Time Discretization Methods*, SIAM J. Numer. Anal., vol. 40, no. 2, pp. 469–491, Jan. 2002,
DOI: 10.1137/S0036142901389025;

[19] D. Dutykh, T. Katsaounis, and D. Mitsotakis (2011), *Finite volume schemes for dispersive wave propagation and runup*, Journal of Computational Physics, vol. 230, no. 8, pp. 3035–3061, Apr. 2011,
DOI: 10.1016/j.jcp.2011.01.003;

[20] J. T. Kirby, G. Wei, Q. Chen, A. B. Kenedy, and R. A. Dalrymple (1998), *Fully Nonlinear Boussinesq Wave Model. User's Manual, CACR Report no. 98-06*, Center for Applied Coastal Research, Univ. of Delaware, 1998;

[21] G. Wei, J. T. Kirby, S. T. Grilli, and R. Subramanya (1995), *A fully nonlinear Boussinesq model for surface waves. Part 1. Highly nonlinear unsteady waves*, *J. Fluid Mech.*, vol. 294, pp. 71–92, Jul. 1995,
DOI: 10.1017/S0022112095002813;

[22] V. K. Pham, V. N. Vu, and C. Lee (2020), *Numerical simulation of tsunami due to submarine landslide using extended Boussinesq equations*, Proceedings of the 10th International Conference on Asian and Pacific Coasts (APAC 2019) Hanoi, Vietnam, September 25-28, 2019, 2020;

[23] S. A. Rzadkiewicz, C. Mariotti, and P. Heinrich (1997), *Numerical Simulation of Submarine Landslides and Their Hydraulic Effects*, Journal of Waterway, Port, Coastal, and Ocean Engineering, vol. 123, no. 4, pp. 149–157, Jul. 1997,
DOI:10.1061/(ASCE)0733-950X(1997)123:4(149);

Acknowledgment: This research was supported by a grant (code 20CTAP-C151982-02) from the Technology Advancement Research Program (TARP) funded by the Ministry of Land, Infrastructure, and Transport of the Korean government.

Received: April 6, 2021
Reviewed: April 9, 2021
Revised: May 1, 2021
Accepted: May 7, 2021